北海道大学工学部研究報告
第158号（平成4年）

Bulletin of the Faculty of Engineering
Hokkaido University No. 158 (1992)

Bound - State Solutions for One - Dimensional Periodic Potential with Multiple Barriers per Period

Yutaka ABE
(Received November 1, 1991)

Laboratory of Quantum Instrumentation,
Faculty of Engineering, Hokkaido University,
Sapporo, 060, JAPAN

Abstract

The energy bands of electrons in a one-dimensional periodic potential consisting of multiple rectangular barriers and wells per period are calculated using transfer matrix method. It is shown that the energy bands can be derived from the reflection and transmission ampulitudes of the individual rectangular barriers and can be easily extended to the cases of complex configurations of barriers and wells in the unit cell. The numerical results suggest the possibility of new type of superlattice devices composed by two different quantum-wells inside the unit cell.

1. Introduction

Advanced technology in the expitaxial growth of semiconductor heterostructures has made possible the structures of coupled multi-layers of quantum-well, which is called a superlattice. Recently, the properties of these superlattices have been studied intensively[1]. The characteristic features of the band structure of such supperlattice are generally discussed in terms of the Kronig-Penny model[2]. The relation between a finite number of layers in the superlattice and the Kronig-Penny model has been discussed by Kolbas and Holonyak[3], and it was shown that a few number of coupled wells have bound electronic states which were well explained by Kronig-Penny model.

In this paper, we investigate the energy band structure of an electron in an one-dimensional periodic potential consisting of multiple barriers per unit cell, using transfer matrix method[4]. We have shown in what manner the band structure can be modified artificially by changing the heights of potentials and the relative position of individual barriers inside the unit cell. The calculated results indicate a new possibility to design superlattices which have the desired energy gaps and the dispersion relations.

2. Multiple barriers per pemiod

The general periodic potential with multiple barriers per period is schematically shown in Fig 1. The unit cell, in this case, contains a multiple number of A-type potentials and B-type potentials.

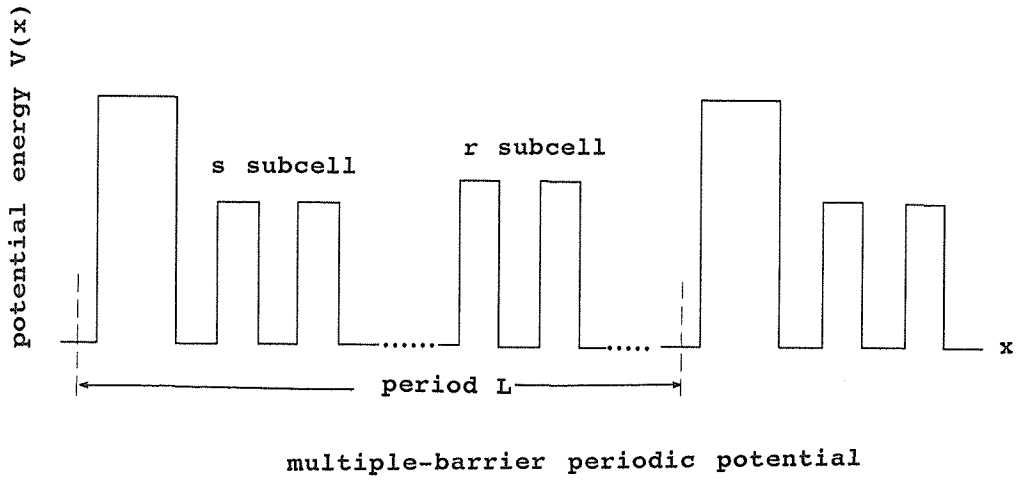

Fig. 1 An one - dimensional periodic potential involved complex subcell per unit cell.

Schroedinger wave equation for an one-dimensional potentials is written by

$$[-(\hbar^2/2\,m)d^2/dx^2+V(x)]\Psi(x)=E\Psi(x) \quad (1).$$

At the n cell boundaries, the general solution to Eq. (1), can be given by

$$\Psi(x)=A_n \exp[i\alpha_n(x)x]+B_n \exp[-i\alpha_n(x)x] \quad (2).$$

Since the wave functions in a periodic potential must satisfy the Bloch condition, Eq. (1) must have the form

$$\Psi(x)=U_k(x)\exp(ikx) \quad (3).$$

and, $U_k(x)$ is expressed as

$$U_k(x)=A_n \exp[i(\alpha_n-k)x]+B_n \exp[-i(\alpha_n+k)x] \quad (4\,a).$$

where $\alpha_n=\alpha_n(x)$. $U_k(x)$ must also have the same period l as V(x), and

$$U_k(x)=U_k(x+ml),\ m=0,\pm1,\pm2,\cdots \quad (4\,b).$$

Use of Eq. (3a) and (3b) at x and x-l, we obtain

$$A_{n-1}\exp[i(\alpha_{n-1}-k)x]+B_{n-1}\exp[-i(\alpha_{n-1}-k)x]$$
$$=A_n \exp[i(\alpha_n-k)\,(x-1)]+B_n \exp[-i(\alpha_n-k)\,(x-1)]. \quad (5).$$

For Eq. (4) to be true for all x, the following relations must be satisfied:

$$\begin{pmatrix}A_n\\B_n\end{pmatrix}=\begin{pmatrix}\exp[-i(\alpha_n-k)1] & 0\\ 0 & \exp[i(\alpha_n+k)1]\end{pmatrix}\begin{pmatrix}A_{n-1}\\B_{n-1}\end{pmatrix}=\mathbf{T}\begin{pmatrix}A_{n-1}\\B_{n-1}\end{pmatrix} \quad (6).$$

Now, let us focus our attention on the subcell inside the unit cell. The pth subcell and (p-1) th subcell in the (n-1) th unit cell must also be related through a transfer matrix, p_m, by the relation

$$\begin{pmatrix}A_{n-1,\,p}\\B_{n-1,\,p}\end{pmatrix}=\mathbf{P}_m\begin{pmatrix}A_{n-1,\,p-1}\\B_{n-1,\,p-1}\end{pmatrix} \quad (7).$$

If the subcells consist of s A-type potentials and r B-type potentials, Eq. (7) can be expressed as

$$\begin{pmatrix} A_n \\ B_n \end{pmatrix} = \underbrace{\mathbf{P}_B \mathbf{P}_B \mathbf{P}_B \cdots\cdots}_{S \text{ times}} \underbrace{\mathbf{P}_A \mathbf{P}_A \mathbf{P}_A \cdots\cdots}_{r \text{ times}} \begin{pmatrix} A_{n-1} \\ B_{n-1} \end{pmatrix} = \mathbf{P} \begin{pmatrix} A_{n-1} \\ B_{n-1} \end{pmatrix} \quad (8).$$

where

$$\mathbf{P} = \mathbf{P}_B{}^S \mathbf{P}_A{}^r \quad (9).$$

The characteristic equation for the allowed electron energy is obtained by the following determinant:

$$[\mathbf{P} - \mathbf{T}] = 0 \quad (10).$$

2-1. Application to the monoatomic potential chain

In the first place, let us consider a simple one-dimensional potential array as shown in Fig. 2. The model for this type of periodic potential is well known as a "Kronig -Penny" model.

The Bloch functions, U_1, corresponding to a electron-wave travelling to the right is given by

$$U_1 = A\,1 \exp[i(\alpha - k)x] \times B\,1 \exp[-i(\alpha + k)x] \quad x < 0 \quad (11\,a).$$

$$c\,1 \exp[(\beta - ik)x] + c\,2 \exp[-\beta + ik)x], \; 0 < x < 1 \quad (11\,b).$$

$$= t \exp[i(\alpha - k)x], \; x > a \quad (11\,c).$$

where

$\hbar\alpha = (2\,m\,E)^{0.5}$ and $\hbar\beta = [2\,m(V_a - E)]^{0.5}$.

With Eq. (11a) and Eq. (11c) at $x=0$ and $x=a$, we have

$$\begin{pmatrix} t \\ 0 \end{pmatrix} = \begin{pmatrix} P_{11} & P_{12} \\ P_{21} & P_{22} \end{pmatrix} \begin{pmatrix} 1 \\ r \end{pmatrix} \quad (12).$$

For the electron traveling wave to the left, the Bloch functions have the following forms:

$$U_2 = r \exp[i(\alpha - k)x] + \exp[-i(\alpha + k)x], \; x > a \quad (13\,a).$$

$$= f \exp[\beta - ik)x] + g \exp[-(\beta + ik)x], \; 0 < x < a, \quad (13\,b).$$

$$= t \exp[-i(\alpha + k)x], \; x < 0 \quad (13\,c).$$

With the same procedures mentioned above, we obtain the following matrix equa-

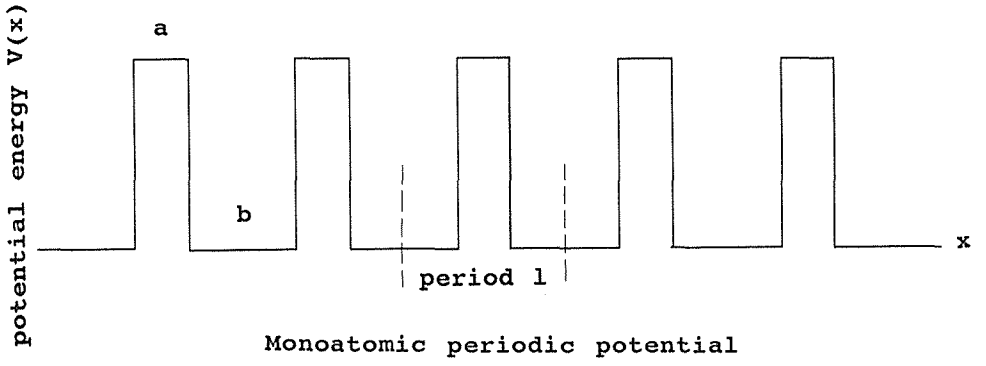

Fig. 2 A simple monoatomic potential array.

tion:

$$\begin{pmatrix} r \\ 1 \end{pmatrix} = \begin{pmatrix} P_{11} & P_{12} \\ P_{21} & P_{22} \end{pmatrix} \begin{pmatrix} 0 \\ t \end{pmatrix} \tag{14}$$

For real eigenvalues of E, the time-reversal property of the Schroedinger equation yields[4]

$$P_{11}=(t^2-r^2)/t, \qquad P_{12}=r/t,$$
$$P_{21}=-r/t, \qquad P_{22}=1/t, \tag{15}$$

where the asterisk denotes the complex conjugate. The P is written as

$$P_{11}{}^*=P_{22},$$
$$P_{12} =P_{21}{}^* \tag{16}$$

The r and t can be derermined from Eqs. (12a)-(12c) using the boundary conditions that U_1 and its derivative are continuous at x=0 and x=a, and are given by

$$\mathbf{P}=\begin{pmatrix} 1/t^* & r/t \\ r^*/t^* & 1/t \end{pmatrix} \tag{17}$$

The determinant for the energy eigenvalues becomes

$$r=(\alpha^2+\beta^2)\ \mathrm{Sinh}(\beta a)/R$$
$$R=[(\alpha^2-\beta^2)\ \mathrm{Sinh}(\beta a)+2\,i\alpha\beta\ \mathrm{Cosh}(\beta a)$$
$$t=-2\,i\alpha\beta/T$$
$$T=\exp(i\alpha a)\ [(\alpha^2-\beta^2)\ \mathrm{Sinh}(\beta a)+2\,i\alpha\beta\ \mathrm{Cosh}(\beta a) \tag{18}$$

The determinant for the energy eigenvalues becomes

$$\begin{bmatrix} (1/t^*)-\exp[-i(\alpha-k)\ (a+b)] & r/t \\ r^*/t^* & (1/t)-\exp[i(\alpha+k)\ (a+b)] \end{bmatrix}=0 \tag{19}$$

Substituting Eqs (18a) and (18b) into (19), we obtain the famous Kronig-Penny relation:

$$\mathrm{Cos}(k\,1)=\mathrm{Cos}(\alpha b)\mathrm{Cosh}(\beta a)+[(\beta^2-\alpha^2)/2\,\alpha\beta]\mathrm{Sin}(\alpha b)\mathrm{Sinc}(\beta a) \tag{20}$$

There is a more direct, and simpler method for this simple arrangement of lattice atoms, which is described in the most standard textbooks[5]. However, as the configuration of the unit cell becomes complex, the direct method becomes extremely complicated and would be impractical. Typical example of Kronig-Penny band is shown in Fig. 3(a).

The density of states in one-dimension is given by

$$N(E)=(2/\pi)dk/dE \tag{21}$$

and this can be derived from the calculated dipersion relation E(k). As expected, the density of states show the Van Hove singularities at the band edges due to the vanishing of the group velocity, as shown in Fig. 3(b).

The structure of GaAs-GaAlAs-GaAs superlattice is schematically shown in Fig. 4 (a). The band structure of this superlattice based on the Kronig-Penny model are shown in Fig. 4(b), and it is seen that even by one-dimensional treatment, several characteristic features of this band structure can be well understood with this simple model as shown in Fig. 5

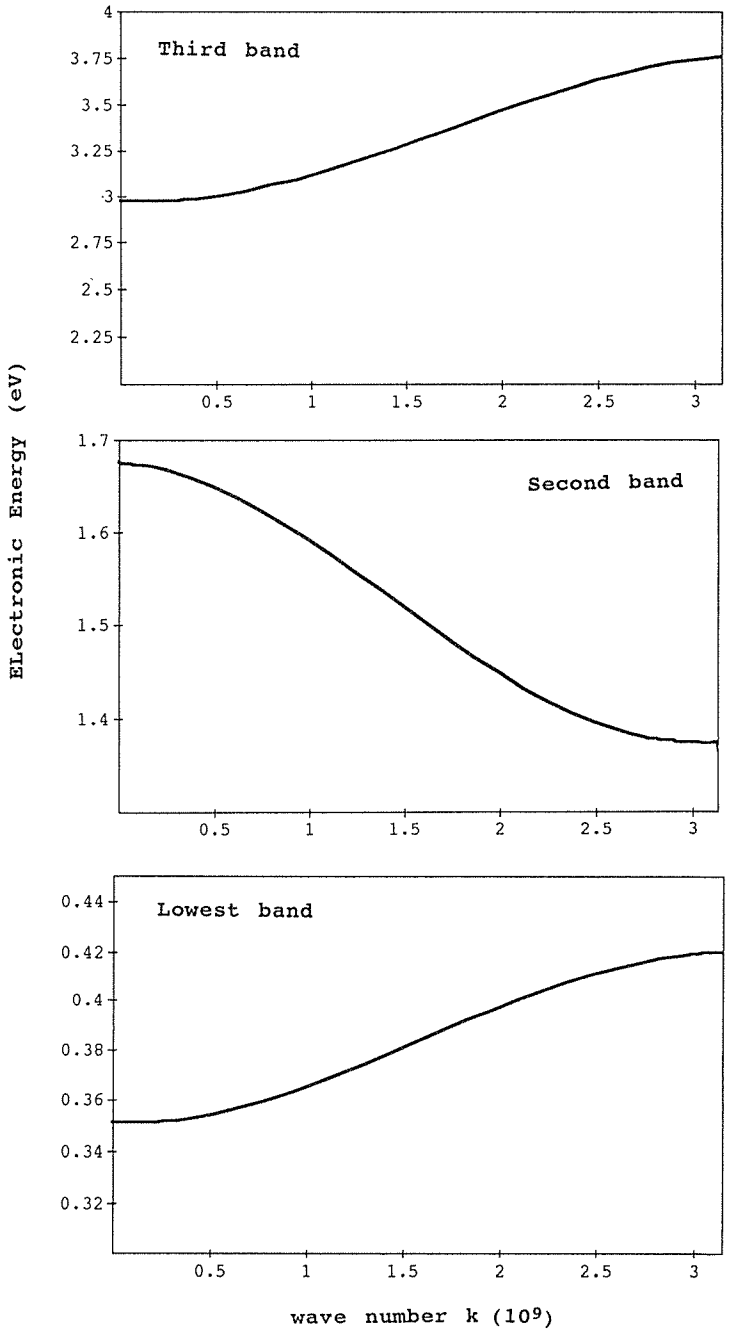

Fig. 3(a) An example of Kronig - Penny Band. V=4.5 eV, a=2 Å, and b=8 Å.

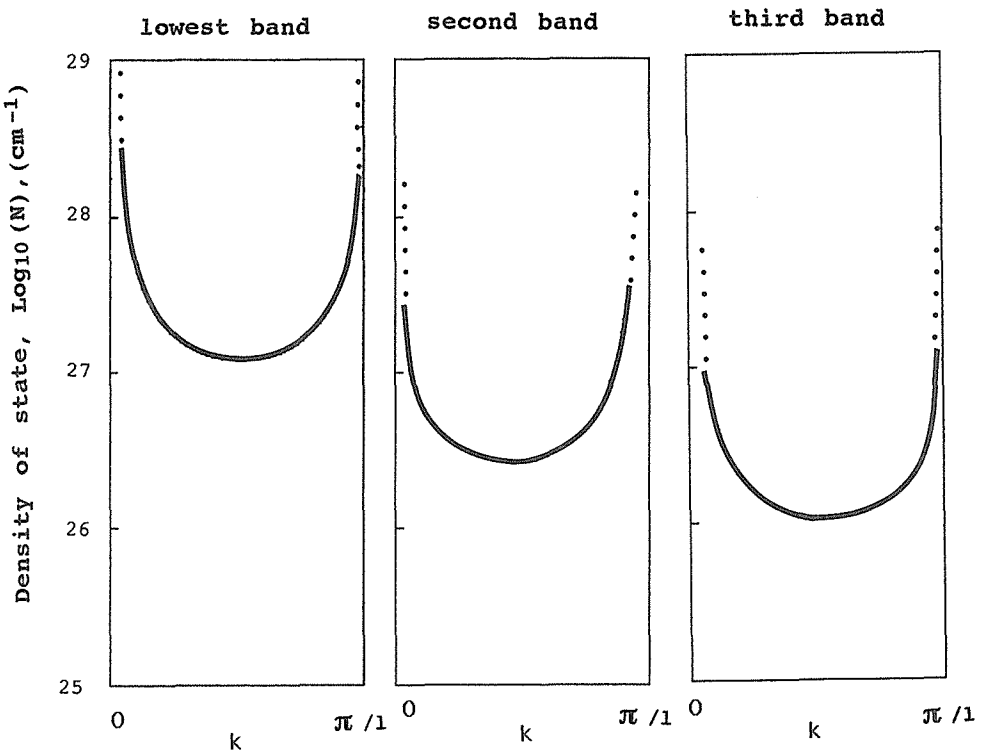

Fig. 3(b) The density of state for the bands in **Fig. 3(a)**0.

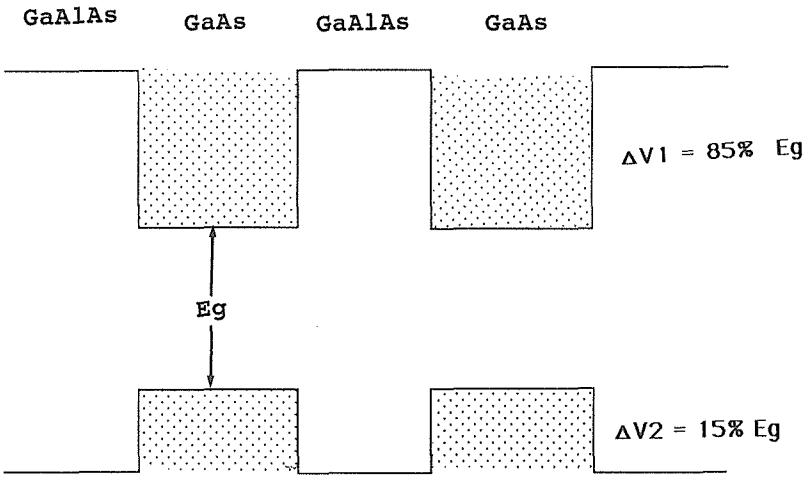

Fig. 4(a) The schematic band structure of GaAlAs - GaAs superlattice.

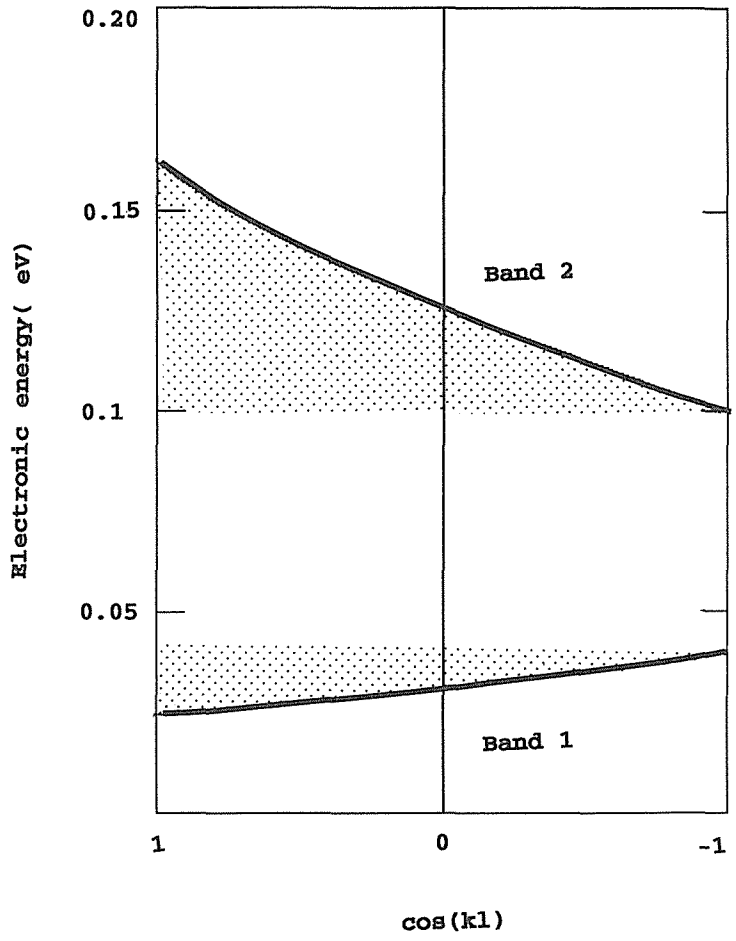

Fig. 4(b) Plot of energy versus cos(kl) of the superlattice. Va=0.25 eV, a=20 Å, and b=100 Å.

2-2. Application to type AB subcell potential arrays

It is straight forward to extend the previous calculations to one-dimensional AB type potental array as shown in Fig. 6.

The basic procedures are: 1) determine P-matrix for each subcell and 2) construct overall P-matrix for subcells, and

3) finally obtain the energy eigenvalues from the characteristic equation $|\mathbf{P}-\mathbf{T}|=0$.

For type A barrier, Pa is

$$\mathbf{P}_a=\begin{pmatrix} 1/t_a^* & r_a/t_a \\ r_a^*/t_a^* & 1/t_a \end{pmatrix}=\begin{pmatrix} p_a^* & q_a \\ q_a^* & p_a \end{pmatrix} \quad (22\,a),$$

and for type B barrier, Pb is

$$\mathbf{P}_b=\begin{pmatrix} 1/t_b^* & r_b/t_b \\ r_b^*/t_b^* & 1/t_b \end{pmatrix}=\begin{pmatrix} q_b \\ p_b \end{pmatrix} \quad (22\,b).$$

Each term of p_a, q_a, p_b and q_b are given by

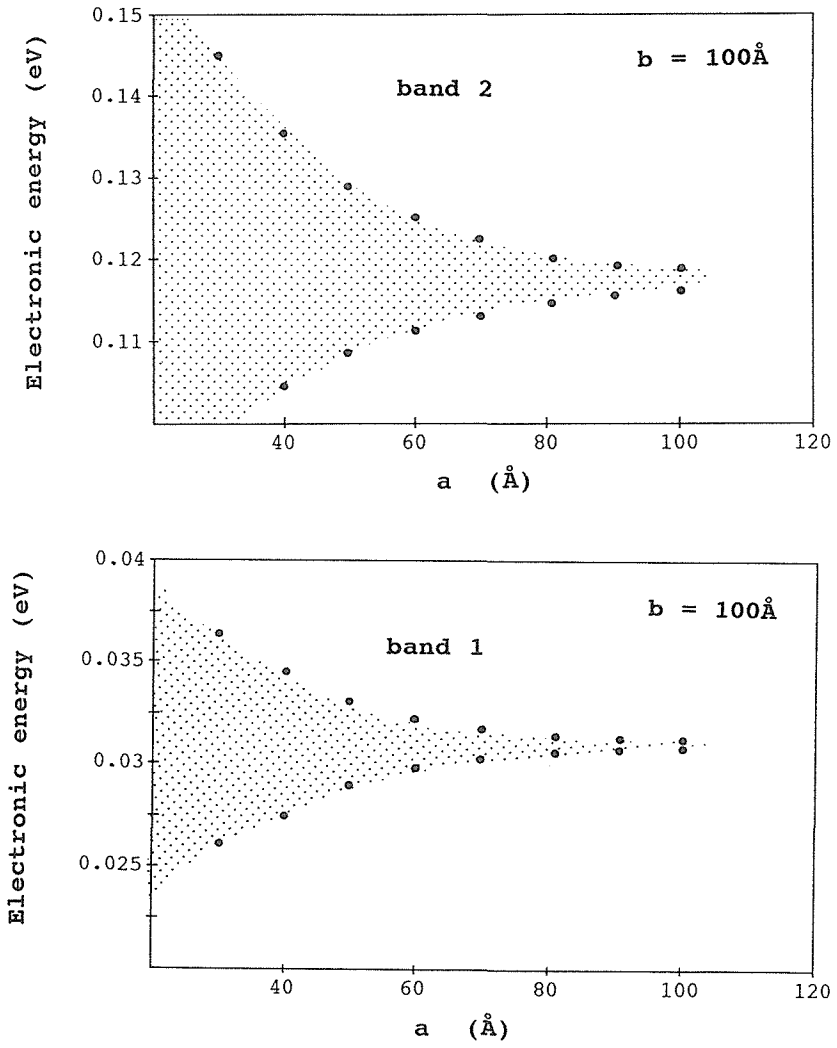

Fig. 5 The variation of the width of conduction band as a function of the width of potential barrier a.

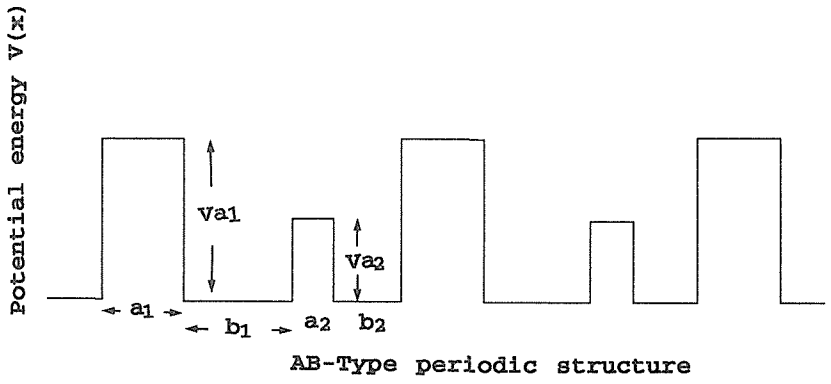

Fig. 6 AB - type subcell potential arrays.

$$p_a = \exp(i\alpha a\,1)\{\mathrm{Cosh}(\beta_1\ a\,1) - i[(\alpha^2-\beta^2)/2\ i\alpha\beta_1]\mathrm{Sinh}(\beta\ 1\ a\ 1)\}$$
$$q_a = -i\exp[i\alpha\ a\,1]\ [\alpha^2+\beta^2)/2\ \alpha\beta_1]\mathrm{Sinh}(\beta_1\ a_1)$$
$$p_b = \exp(i\alpha a\,2)\{\mathrm{Cos}(\beta_2\ a\,2) - i[(\alpha^2-\beta_2^2)/2\ \alpha\beta\ 2]\mathrm{Sinh}(\beta\ 2\ a\ 2)\}$$
$$q_a = -i\exp[i\alpha(a\,1+b\,1+a\,2)]\ [(\alpha^2+\beta^2)/2\ \alpha\beta\ 2]\mathrm{Sinh}(\beta\ 2\ a\ 2) \qquad (23\ a)$$

and

$$\hbar\beta_1 = [2\ m(Va\ 1-E)]^{0.5}$$
$$\hbar\beta_2 = [2\ m(Va\ 2-E)]^{0.5} \qquad (23\ b).$$

The final determinant is

$$\begin{bmatrix} w\ 11-\exp[-i(\alpha-k)1 & w\ 12 \\ w\ 21 & w\ 22-\exp[i(\alpha+k)1] \end{bmatrix} = 0 \qquad (24\ a),$$

where

$$w\ 11 = p_b{}^* p_a{}^* + q_b\ q_a$$
$$w\ 12 = p_b{}^*\ q_a + q_b\ p_a$$
$$w\ 21 = q_b{}^*\ p_a{}^* + p_b\ q_a{}^*$$
$$w\ 22 = q_b{}^*\ q_a + p_b\ p_a \qquad (24\ b).$$

The explicit relation for the energy eigen values are: For E<Val and Va2,

$$\mathrm{Cos}(k\ 1) =$$
$$[\mathrm{Cosh}(\beta_1\ a_1)\ \mathrm{Cos}(\beta_2\ a_2) - Q_1\ \mathrm{Sinh}(\beta_1\ a_1)\ \mathrm{Sinh}(\beta_2\ a_2)]$$
$$\times \mathrm{Cos}[\alpha(b_1+b_2)]$$
$$+[Q_2\ \mathrm{Sinh}(\beta_1\ a_1)\ \mathrm{Cosh}(\beta_2\ a_2) + Q_3\ \mathrm{Cosh}(\beta_1\ a_1)\ \mathrm{Sinh}(\beta_2\ a_2)]$$
$$\times \mathrm{Sin}[\alpha(b_1+b_2)]$$
$$+Q_4\ \mathrm{Sinh}(\beta_1\ a_1)\ \mathrm{Sinh}(\beta_2\ a_2)\ \mathrm{Cos}[\alpha(\beta_1-\beta_2)], \qquad (25)$$

where

$$Q_1 = (\beta_1{}^2-\alpha^2)(\beta_2{}^2-\alpha^2)/4\ \alpha^2\beta_1\beta_2$$
$$Q_2 = (\beta_1{}^2-\alpha^2)/2\ \alpha\beta_1$$
$$Q_3 = (\beta_2{}^2-\alpha^2)/2\ \alpha\beta_2$$
$$Q_4 = (\beta_1{}^2+\alpha^2)(\beta_2{}^2+\alpha^2)/4\ \alpha^2\beta_1\beta_2.$$

For Val<E<Va2, the dipersion relation can be derived by substituting $\beta 1 = i\Gamma$ into the Eq. (25), where $\hbar\Gamma = [2m(Val-E)]^{0.5}$.

2-3. Numerical examples and discussion

Equation (25) can be used to obtain the band structure of a superlattice system composed of various configurations of two different quantum-wells and barriers per period. For example, let us consider the GaAs-Ga_{1-x} Al_xAs binary superlattice system. The barrier height can be varied by the content of Al in Ga_{1-x} al_xAs the layer.

Fig. 7 is the plot of energy E(k) versus cos(kl) with l=230 Å, al=50 Å, a2=20 Å, bl=b2=80 Å, Val=0.25eV, and Va2=0.20eV. Comparing this particular choice of the barrier configuration with the simple Kronig-Penny model(a=50 Å, b=180 Å, Va=0.25eV), it may be seen that the each band in Kronig-Penny model are modified due to the additional potential barrier a2. It is interesting to note that the odd numbered bands, band 1 and band 3 in this case, are strongly perturbed while the even numbered bands are

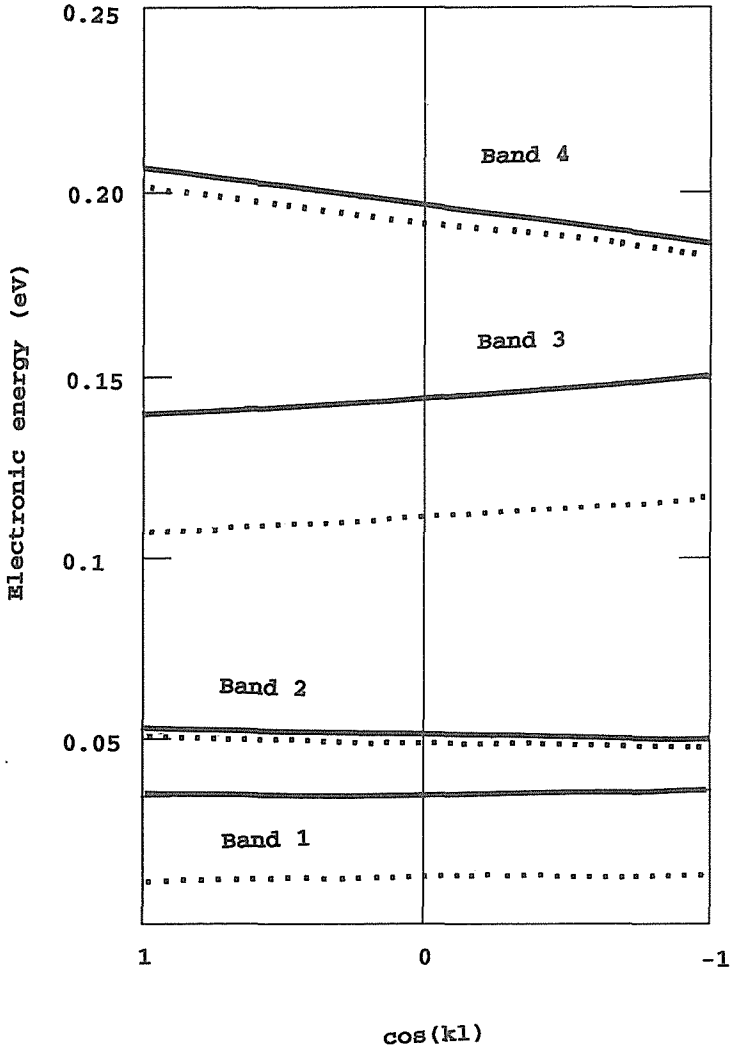

Fig. 7 Numerical results of the band structures in a AB-type superlattice structure. Dotted line is the results of simple Kronig-Penny type bands with a=50 Å, b=180 Å, and Va=0.25 eV.

weakly modified by the additinal potential barrier.

The band gaps and the band width are the functions of the ratio $w=b_2/b_1$ and the electronic energy spectrum can vary over a wide range by changing the ratio w. The actual variations of the energy gaps by the relative position of individual barriers inside the unit cell are shown in Fig. 8. Egl, the energy gap between first band and second band, is increased rapidly with increasing the ratio w and reaches the peak value at around w=3. Further increase of w makes Eg_2 almost saturated. Eg_3, the energy gap between the third band and fourth band, is also increased by increasing the ratio w and reaches its peak value at w=2.4, followed by a rapid decrease with the increasing value

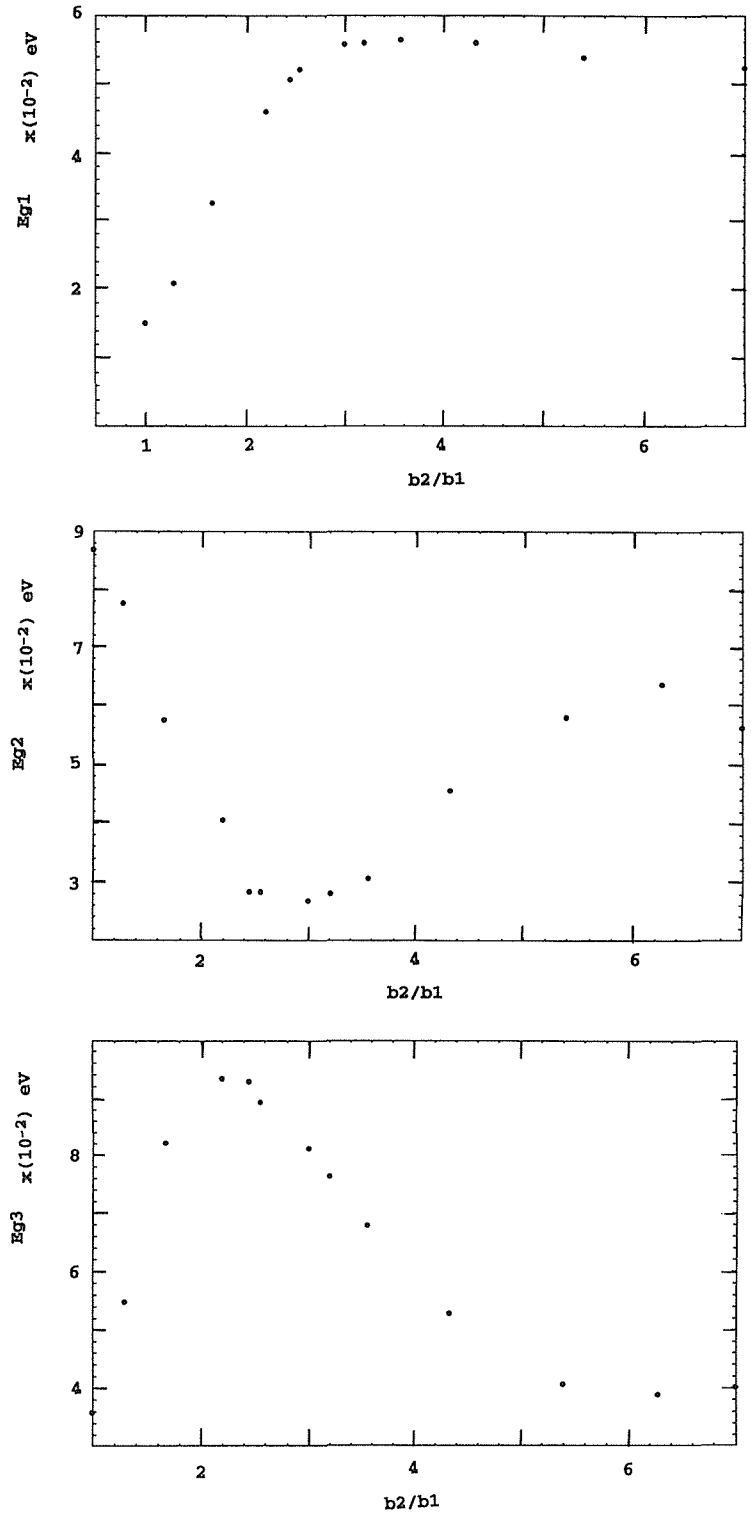

Fig. 8(a), (b), and (c) Variations of energy gaps as a function of the ratio $w=b_2/b_1$.

of w. Eg_2, the energy gap between the second band and third band, shows a rather complex behavior. Eg2 has its minimum value at w=3.0 and the peak value at w= 6.2 in this case.

When the additional barrier is located at an asymmetric position in the unit cell, the wavefunctions in the narrow-well are more localized, namely more tightly bound to the local potential, while the wavefunctions in the residual part of the unit cell become more extended. Although the characteristic feature such as resonant scattering in a single barrier is smeared out in the arrangement of a periodic potential, the mutually contradicted nature of the wavefunctions mentioned above may reflect the actual band structures and the complex variations of energy gaps may arise.

The band width of the each band also depends on the relative positions of two bar-

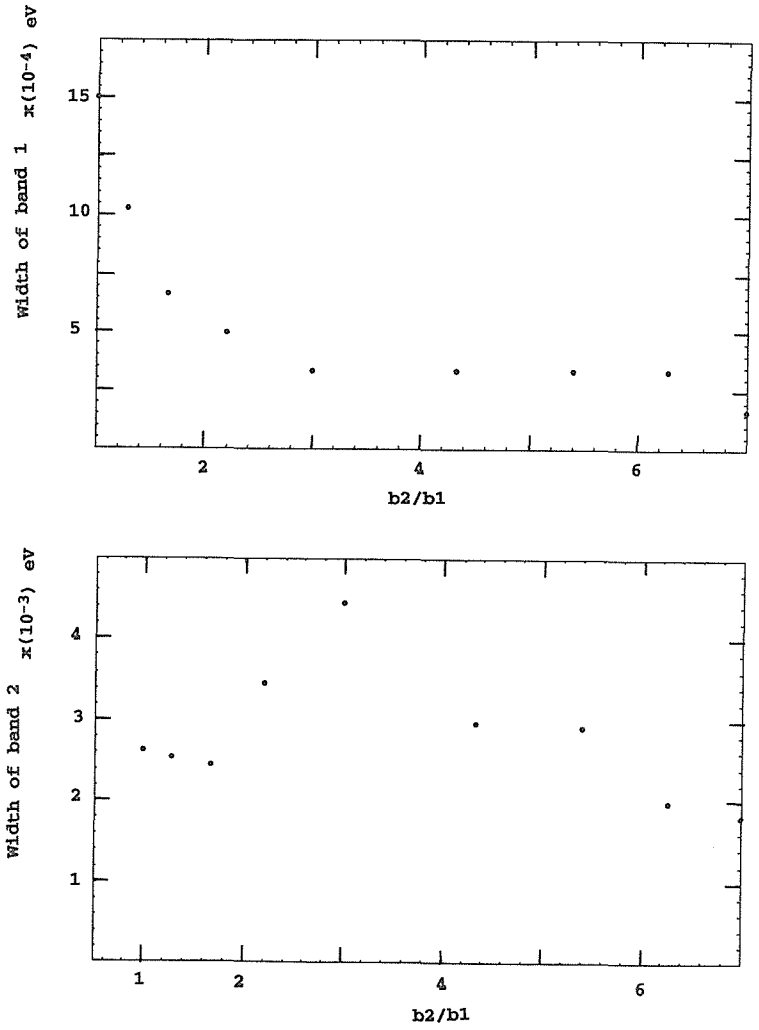

Fig. 9(a) and (b) Variations of the bandwidths as a function of the ratio w.

riers in the unit cell and this feature is shown explicitly in Fig. 9. The band width is considered to be determined by the transfer integral and the tranfer intergral depends explicity on the width of the well. The similar contradictory interaction in the transfer integral in the asymmetric quantum-wells inside the unit cell will also happen in this case, and this causes the complex dependence of the width on the ratio w.

The similar features of the modification of band structures as described in the above section are also found in the case of V1a < V2a.

3. Concluding remarks

It is shown that the band structure of superlattices with multiple barriers in a unit cell can be calculated by elementary but a systematic method using a transfer matrix. We did not take into account the variation of the effective mass along the vertical quantum-well of a different constituent. As long as the difference of the variation of constituent between subcells are small, the results of the present calculations may be well approximated the real superlattice band structures.

Our results suggest that the new type of infrared detector and laser which is based on the AB type superlattice. The wide variaty of energy gaps can be obtained by the variation of individual barrier heights and the relative position of each barrier in a unit cell.

The Bloch oscillation in superlattices under the high electric field greater than $h/qa\tau$, where q is the electronic charge and τ is the relaxation time, is one of the challenging targets in applications of superlattice structures. The difficulty of obseving such oscillations stems from the fact that the field must be very high and this field causes transitions of electrons into a hiqher miniband by tunneling and this transition supresses Bloch oscillation. As shown in the previous section, the energy gap between the first band and the next excited band can be increased with suitable configuration of AB potential barriers in the unit cell, and this suggests a new approach to the realization of Bloch oscillator.

The strains between the quantum-well layers composed of different atomic constituents change definitely the bulk properties of each layer and further refinement of the present treatment is necessary to obtain the rigorous results including the effect of the strain.

References

1) Geral Bastard, Wave mechanics applied to semiconductor heterostructures, (Halsted Press, New York) 1988. Detailed references for heterostructures and superlattices are cited in the context.
2) L. L. Chang, L. Esaki, and R. Tsu, Appl. Phys. Lett. 24, 593 (1974).
3) R. M. Kolbas and N. Holonyak, Jr., Am. J. Phys. 52, 431, (1984).
4) E. Merzubacher, Quantum Mechanics (Wiley, New York, 1970), 2nd ed., pp 80-105.
5) C. Kittel, Introduction to Solid State Physics (Wiley, New York, 1976), 5th ed., pp. 191-193.